

# Neuroprotectin D1 Protects Against Postoperative Delirium-like Behaviors in Aged Mice by Regulating Neuroinflammation Induced by Surgical Trauma

Ying Zhou

Wuhan University Zhongnan Hospital <https://orcid.org/0000-0003-1040-1089>

Jiayu Wang

Wuhan University Zhongnan Hospital

Xiaofeng Li

Wuhan University Zhongnan Hospital

Ke Li

Wuhan University Zhongnan Hospital

Lei Chen

Wuhan University Zhongnan Hospital

Zongze Zhang

Wuhan University Zhongnan Hospital

Mian Peng (✉ [sophie\\_pm@msn.com](mailto:sophie_pm@msn.com))

---

## Research

**Keywords:** Postoperative delirium, Specialized proresolving lipid mediators, Neuroinflammation, Macrophage polarization

**Posted Date:** May 19th, 2020

**DOI:** <https://doi.org/10.21203/rs.3.rs-28936/v1>

**License:**   This work is licensed under a Creative Commons Attribution 4.0 International License.

[Read Full License](#)

---

# Abstract

## Background

Postoperative delirium (POD) is the most common postoperative complication affected elderly patients, yet the underlying mechanism is elusive and without effective therapy. The neuroinflammation hypothesis has been emerging as the pathogenesis of POD. Recently, accumulative evidence has supported the role of specialized proresolving lipid mediators (SPMs) in regulating inflammation. NPD1, a novel member of SPMs, is identified with potent immune-resolvent and neuroprotective effect. We aimed to investigate the role of NPD1 in neuroinflammation and postoperative cognitive function with a mice model of POD.

## Methods

Aged male C57BL/6 mice were subjected to laparotomy under isoflurane anesthesia with NPD1 prophylaxis. The general and memory behaviors were assessed by buried food test, open field test and Y maze test at 6, 9, and 24 hours after the surgery. Expression level of inflammatory cytokines were analyzed by ELISA. The permeability of blood-brain barrier (BBB) was detected by spectrophotometric quantification of extravascular dextran tracer from brain tissue extracts, and the expression of tight junction (TJ) associated proteins by Western blotting. The reactive states of astrocytes and microglia were examined by immunofluorescence. The protective effects of NPD1 was also evaluated through macrophage polarization by flow cytometry, using the bone marrow-derived macrophages cultures.

## Results

NPD1 prophylaxis decreased the expression of pro-inflammatory cytokines and increased the expression of anti-inflammatory cytokines in peripheral blood, hippocampus and prefrontal cortex, and limited the leakage of BBB by increasing the expression of TJ associated proteins. Besides, NPD1 prevented the activation of microglia and astrocytes both in the hippocampus and prefrontal cortex, which resulted in improved general and memory function of mice. Furthermore, NPD1 treatment modulated the inflammatory cytokine profile and promoted the macrophage polarization toward M2 in LPS-stimulated macrophages.

## Conclusions

These findings verify the anti-inflammatory and proresolving activities of NPD1 in the inflammatory milieu both *in vivo* and *in vitro*, and provide better insight into the pathophysiology and potential therapy for POD.

# Background

Postoperative delirium (POD), defined as delirium occurring mainly within 1 week after surgery, is a common neuropsychiatric complication characterized by fluctuating and concurrent disturbances of attention, cognition, psychomotor behavior, emotion and sleep-wake rhythm. POD has been linked to higher mortality, prolonged hospitalization, increased risk of long term cognitive impairment [1, 2], and presents with extra medical burden on governments and society [1, 3]. The incidence of POD is ranged from 14% in the general medical units to 82% in the intensive care unit, particularly with higher tendency in elderly patients [4–6]. As aging has become a common issue in global, the number of elderly who need surgery/anesthesia treatment has been increasing, as well as the prevalence of POD. However, there are no effective therapies for this complication for the undefined underlying pathophysiology.

Recent studies highlight the importance of neuroinflammation in the development of POD [7, 8]. Surgical trauma activates the innate immune system, leading to the systemic release of cytokines [7]. The humoral pro-inflammatory cytokines, such as tumor necrosis factor (TNF- $\alpha$ ) and interleukin-6 (IL-6), have been reported to be associated with the leakage of the blood-brain barrier (BBB), which leads to the entrance of pro-inflammatory cytokines and monocyte-derived macrophages, resulting in the activation of glia, including microglia and astrocytes [9, 10]. This process is mainly affected by the bone marrow-derived macrophages (BMDMs), which react dually to the microenvironmental cues to initiate the neuroinflammation [11–13]. Interaction between peripheral immune and brain amplifies the inflammation in the central nervous system (CNS) [14, 15], and the cascade of neuroinflammation induces the synaptic dysfunction and neuronal apoptosis, ultimately impairs the cognitive function [16, 17]. On this basis, treatments targeting at reversing neuroinflammation show great potential to be candidate therapies for POD.

Along with passive termination of inflammation, resolution actively participates in the restoration of acute inflammation as a coordinated program, which is regulated by specialized proresolving lipid mediators (SPMs) [18]. SPMs are endogenous biosynthesis from essential fatty acids with potent properties of anti-inflammation and immunoregulation [19, 20]. Protectin D (PD) family, specially termed as neuroprotectin D1 (NPD1) when synthesized in the neural system, is one of the SPMs derived from omega-3-polyunsaturated fatty acid docosahexaenoic acid (DHA), sharing similar biological activities with other lipid mediators such as resolvins and maresins, including accelerating nonphlogistic macrophage phagocytosis, inhibiting neutrophil infiltration and regulating the production of cytokines and chemokines [20–22]. Additionally, NPD1 has been demonstrated to be neuroprotective in the preclinical models of Alzheimer's disease, which shares some characteristics with POD such as memory impairment [23, 24]. However, there are not any reports about the role of NPD1 in the POD.

Based on these discoveries, we proposed the hypothesis that prophylaxis with NPD1 could improve the POD-like behavior of aged mice through its proresolving effect on the inflammation induced by surgical trauma. To validate this hypothesis, we assessed the effects of NPD1 on the postoperative behavior of aged mice, and inflammation events both in the periphery and in CNS. Furthermore, we aimed to

determine that NPD1 exerts anti-inflammatory and proresolving properties by promoting macrophage polarization, which is pivotal in promoting the restorative process in the acute inflammation [25].

## Methods

### Animals

The experimental protocol was approved by the Animal Ethics Committee of Zhongnan Hospital of Wuhan University, and all experiments were performed following the National Institutes of Health Guidelines for the Care and Use of Laboratory Animals. Female C57BL/6 mice (Changsha Tianqin Biotechnology CO., LTD., Changsha, China), 18 months old, and weighing 30–40 g were group-housed 4–5 per cage on a 12-hour light/dark cycle in a temperature-controlled ( $25 \pm 2^\circ\text{C}$ ) room with free access to standard rodent water and food.

### Experimental Protocol

The mice were randomly divided into the control group, surgery group, NPD1 group, or NPD1 + surgery group. NPD1 (Cayman Chemical, Ann Arbor, MI, USA) was given at  $2 \mu\text{g}/\text{ml}$  in saline with 1.4% ethanol, i.p. 600 ng (300  $\mu\text{l}$ ) per mouse in NPD1 group and NPD1 + surgery group, while the equal volume of 1.4% ethanol in saline was given in control group and surgery group. One hour after administration of NPD1 or vehicle, mice in the surgery group and NPD1 + surgery group were subjected to a simple laparotomy under isoflurane anesthesia, while the mice in the control group and NPD1 group were placed in their home cages with 100% oxygen for two hours without surgery treatments. The mice had multiple behavioral tests at 24 hours before the surgery (baseline), and at 6, 9, and 24 hours after the surgery/anesthesia. Within each group, separate cohorts were subjected to assessment at each time point ( $n = 8–10$  per cohort). To measure BBB permeability by immunohistochemistry and spectrophotometric quantification, mice were given with 10-kDa dextran i.v. at 6 hours after surgery/anesthesia, and decapitated 15 min later to harvest the brain ( $n = 5$  per cohort). To detect inflammatory cytokine, mice were sacrificed at 6, 9, and 24 hours after the surgery/anesthesia to collect blood, hippocampus, and prefrontal cortex for Western blotting and ELISA ( $n = 5$  per cohort). At 24 hours postoperatively, mice were anesthetized and transcardially perfused with ice-cold phosphate-buffered saline (PBS) followed by 4% paraformaldehyde. Then, hippocampal and prefrontal cortex tissues were collected for immunostaining ( $n = 3–5$  per cohort).

### Surgical Model

A simple laparotomy was performed under isoflurane anesthesia using the methods as described in our previous studies [26, 27]. Specifically, each mouse was induced with 1.4% isoflurane in 100% oxygen in a transparent acrylic chamber. Fifteen minutes after induction, the mouse was moved out of the chamber and placed on a heating pad to maintain body temperature between  $36^\circ\text{C}$  to  $37^\circ\text{C}$  during the surgery. Isoflurane anesthesia was maintained via a cone device with a 16-gauge needle sensor monitoring the

concentration of isoflurane. A longitudinal midline incision was made from the xiphoid to the 0.5 cm proximal pubic symphysis on the skin, abdominal muscles and peritoneum. Abdominal organs were partially exposed for 2 min, then the incision was sutured layer by layer with 5 – 0 Vicryl thread. The procedure for each mouse lasted about 10 minutes, then the mouse was put back into the anesthesia chamber for up to 2 hours to receive the rest of the anesthesia. Blood pressure was monitored with the mouse-tail blood pressure cuff (Softron BP-2010A, Softron Beijing Biotechnology Co., Ltd., Beijing, China), and blood gas and blood glucose levels were tested by a blood gas analyzer (i-STAT, Abbott Point of Care Inc., Princeton, NJ, USA). Analgesia was given 5 min before skin incision, at the end of the procedure and every 8 hours for one day postoperatively with EMLA cream (2.5% lidocaine and 2.5% prilocaine).

## Behavioral Tests

The behavioral changes were detected by multiple behavioral tests in the order of buried food test, open field test and Y maze test at 24 hours before the surgery, and at 6, 9, and 24 hours after the surgery as described in our previous studies [26]. In all the tests each apparatus was cleaned with 75% ethanol after each mouse to remove odors.

Firstly, for buried food test, each mouse was given 2 pieces of sweetened cereal two days before the test in their home cage. Mice were habituated for one hour before the test by placing the home cage with mice in the testing room. The test cage was contained 3 cm deep of clean bedding and a piece of sweetened cereal pellet buried underneath 0.5 cm below the surface. The location of the food pellet was randomly changed every time. The mouse was placed in the center of the test cage for 5 minutes, and the latency to eat the food was measured as the time interval from the mouse placed in the test cage to when it uncovered the food pellet and grasped it in the forepaws and/or teeth. If the mouse failed to find the pellet within 5 minutes, the latency was defined as 300 seconds.

Secondly, for open field test, mouse was placed in the center of an open field chamber (40 × 40 × 40 centimeters) in a quiet and illuminated room and allowed to freely explore for 5 minutes. The movement parameters of the mouse were monitored and analyzed via a video camera connected to the Any-Maze animal tracking system software (Xinruan Information Technology Co. Ltd., Shanghai, China). Parameters of total distance moved, freezing time and time spent in the center were recorded and analyzed.

At last, the Y maze test was executed in a two trials task in a quiet and illuminated room, with the apparatus consists of three arms (width 8 cm × length 30 cm × height 15 cm) at 120° angles extending from a central space, and each wall of the arms were pasted with cardboards in different patterns as spatial cues. Three arms of Y maze were randomly distributed into the novel arm, which is blocked at the first trial but opened at the second trial; start arm, in which the mouse starts to explore; and another arm, which is always open. The first trial is the training trial which allowed the mouse to explore the start arm and the other arm for 10 minutes, with the novel arm being blocked. After 2 h (for the tests of 6 and 24 hours after surgery) or 4 hours (for the tests of 9 hours after surgery) time interval, the second trial as the

retention trial was conducted. The mouse was placed back in the maze in the same start arm with free access to all the 3 arms for 5 minutes. A video camera, which was linked to the Any-Maze animal tracking system software, was installed 200 centimeters above the chamber to monitor and analyze the number of entries and the time spent in each arm.

## Bbb Permeability Assay

The method is based on the established BBB dye-injection assay with slight modification [28, 29]. Specifically, 6 h after surgery, each mouse was injected intravenously through tail veins with 100  $\mu$ l 10-kDa dextran Texas Red (Invitrogen, D1863). Fifty minutes after injection, each mouse was anesthetized and decapitated. The brains were harvested and fixed by immersion in 4% paraformaldehyde overnight at 4 °C, then cryopreserved in 30% sucrose and frozen in TissueTek OCT (Sakura). Frozen sections of 20  $\mu$ m were collected and post-fixed in 4% PFA at room temperature (20–25 °C) for 15 min, washed in PBS and were blocked with 10% goat serum (Boster Biologic Technology, China) for 2 hours, permeabilized with 0.5% Triton X-100, then incubated with isolectin B4 (20  $\mu$ g/ml, I21411, Molecular Probes, San Francisco, CA, USA) for immunostaining to visualize blood vessels. The fluorescence images of the injected tracer and isolectin were detected under 40 $\times$  objective lens.

Spectrophotometric quantification of extravascular 10-kDa dextran Texas Red was carried out with extracts of the hippocampus and prefrontal cortex at 6 hours after surgery. Specifically, anesthetized animals were perfused transcardially for 5 min with 50 ml PBS, then the brains were removed and homogenized in 1% Triton X-100 in PBS (100  $\mu$ l/100 mg brain tissue). Brain lysates were centrifuged at 16,000 r.p.m. for 20 min and the relative fluorescence of the supernatant was measured on a fluorometer POLARstar Omega (BMG Labtech) (ex/em 595/615 nm).

## Western Blot Analysis

The total protein samples from hippocampal and prefrontal tissues were homogenized using RIPA lysis buffer (150 mM NaCl, 1 mM EDTA, 50 mM Tris, 1% Triton, 0.1% sodium dodecyl sulfate, and 0.5% deoxycholate) containing protease and phosphatase inhibitors. The lysate was centrifuged at 12,000 rpm for 5 minutes at 4 °C to remove the sediment. The supernatants were collected, and the protein concentration was determined by a bicinchoninic acid (BCA) protein assay kit (Aspen, Wuhan, China). After the determination of the contents, the proteins were separated by SDS-PAGE (8–12%) and then transferred to PVDF membranes (Aspen, Wuhan, China). After being blocked with 5% skim milk for 1 hour at room temperature, the membranes were incubated overnight at 4 °C with the following primary antibodies: anti-ZO-1 (1:500, Abcam, ab96587), anti-occludin (1:2000, Abcam, ab167161), anti-claudin-5 (1:500, Biorbyt, orb214680), anti- $\beta$ -actin (1:10,000, TDY Biotech, ab37168). The membranes were washed three times with TBST (20 mM Tris-HCl, 150 mM NaCl, and 0.05% Tween-20) and incubated with horseradish peroxidase-conjugated goat anti-rabbit IgG secondary antibody (Aspen, AS1107) for 30 minutes at room temperature. Specific immunoreactivity was detected using enhanced

chemiluminescence (Aspen, Wuhan, China). The bands were measured using image analysis software (AlphaEaseFC software).

## Enzyme-linked Immune-sorbent Assay (elisa)

The concentrations of TNF- $\alpha$ , IL-6, IL-10, IL-12 in the plasma and brain tissue of mice or the primary bone marrow-derived macrophages for *in vitro* experiments were determined using ELISA kits (eBioscience) according to the manufacturer's instructions.

## Immunofluorescence

At 24 hours after surgery, mice were deeply anesthesia with isoflurane and perfused transcardially with ice-cold 0.1 M PBS followed by 4% PFA in 0.1 M PBS at pH 7.4. Brains were harvested and post-fixed in 4% PFA in 0.1M PBS at 4 °C, and cryoprotected in 30% sucrose for 72 hours. Brains were freeze-mounted in TissueTek OCT (Sakura), and were cut sequentially to 20  $\mu$ m. After washed in PBS and permeabilized in 0.5% Triton X-100, the coronal sections were blocked with 10% goat serum in PBS for 2 hours at room temperature to block non-specific binding, then the following primary antibodies were used: mouse anti-glial fibrillary acidic protein (GFAP) (1:500, Abcam, I21411), rabbit anti-Iba-1 (1:200, Abcam, ab178847) at 4 °C overnight. For secondary detection, (goat anti-mouse, goat anti-rabbit) conjugated with Alexa Fluor dyes (405 and 488) from Invitrogen (1:500) were used. Immunolabelled sections were coverslipped with 40,6-diamidino-2-phenylindole (DAPI; Invitrogen) and visualized by microscopy (Olympus, Tokyo, Japan). Five high magnifications were chosen in three non-overlapping fields randomly acquired in hippocampal subregions using a counting frame size of 0.4 mm<sup>2</sup>. Images were processed and the area of the astrocytes and microglia quantified using ImageJ software (NIH). The area of the selected cells was converted into a binary image using the dilation method and the cell outline measured. Total immunoreactivity was calculated as percentage area density defined as the number of pixels (positively stained areas) divided by the total number of pixels (sum of positively and negatively stained area) in the imaged field.

## Primary Cell Culture And Grouping

Bone marrow-derived macrophages (BMDMs) were purchased from iCell Bioscience Inc (MIC-iCELL-i017, Shanghai, China), and were cultured in DMEM/F-12 containing 10% fetal bovine serum (FBS), 100  $\mu$ g/mL streptomycin, and 100 U/mL penicillin and supplementary factor (iCell Bioscience Inc, PriMed-iCell- 011) 37°C under 5% CO<sub>2</sub> and 95% air. Cells were then stimulated with 10 ng/ml lipopolysaccharide (LPS, Sigma, L2880), with or without NPD1 (80 ng/ml) for 24 h, respectively. The same batches of BMDMs were untreated as control.

# Flow Cytometry Analysis

For cell staining, anti-mouse CD 68-PE, CD16/CD32-PE-Cy7, CD206-PE (Invitrogen) were used. The cells were detached and suspended in flow cytometry staining buffer and treated with Fc-receptor blocker antibody for 20 min at 4 °C to eliminate nonspecific binding. Then the cells were stained by these antibodies for 30 min at 4 °C in dark. After washed twice in flow cytometry staining buffer and resuspended in the staining buffer, samples were detected using a BD FACSCalibur system was used for analysis.

## Statistical analysis

The statistical analyses were performed with SPSS 19.0 (IBM, New York, USA) or GraphPad Prism 6 (GraphPad, New York, USA). Quantitative data are expressed as the means  $\pm$  standard error of the mean (SEM). Statistical significance was determined using 1-way or 2-way analysis of variance, followed by the Bonferroni post hoc test. A *p* value less than 0.05 was considered statistically significant.

## Results

### NPD1 prophylaxis ameliorates POD-like behaviors induced by surgery/anesthesia in aged mice

To determine whether surgery/anesthesia affects general and cognitive behavior of aged mice, we performed a battery of behavioral tests with food buried test, open field test and Y maze test at 24 hours before surgery and 6, 9, 24 hours after surgery in the present study as we previously reported [26, 27].

We first executed the buried food test to explore whether surgery/aesthesia affected the mice's ability to associate odorant with food reward [30]. The latency to eat food was markedly increased in the Surgery group compared to the Control group at 6 hours after surgery ( $P < 0.01$ , Fig. 1A), while pretreatment with NPD1 (600 ng/mouse) improved the impaired ability of finding and eating food induced by surgery/anesthesia ( $P < 0.05$ , Fig. 1A). No significant changes were observed between the NPD1 group and Control group.

Then we executed the open field test to examine the locomotor ability and exploratory behavior of mice with surgery/anesthesia or NPD1 treatment [31]. There were no significant differences in total distance traveled by mice between four groups at any time points, indicating that surgery/anesthesia did not affect the motor function of aged mice (Fig. 1B). Surgery/anesthesia significantly decreased the time spent in the center at 6 and 9 hours after surgery ( $P < 0.05$ ), and preemptive administration of NPD1 ameliorated this phenomenon at 9 hours after surgery ( $P < 0.05$ , Fig. 1C). Besides, surgery/anesthesia significantly decreased the freezing time at 6, 9, 24 hours after surgery ( $P < 0.05$ , Fig. 1D), while preoperative treatment with NPD1 increased the freezing time at 9 and 24 hours after surgery ( $P < 0.05$ ,

Fig. 1D). NPD1 administration alone did not change these parameters compared to the control condition (Fig. 1B-D).

At last we conducted Y maze for assessing the hippocampus-dependent spatial memory in aged mice as previously validated [32]. Surgery/anesthesia did not alter the number of arm visits among four groups (Fig. 1E). However, surgery/anesthesia significantly reduced the number of entries in the novel arm at 6 hours after surgery ( $P < 0.05$ , Fig. 1F) and the duration in the novel arm at 6 and 9 hours after surgery ( $P < 0.05$ , Fig. 1G), as compared to the control condition. Pretreatment with NPD1 increased the number of entries in the novel arm and duration in the novel arm at 6 hours after surgery ( $P < 0.05$ , Fig. 1F-G). NPD1 administration *per se* did not affect the performance of aged mice in the Y maze test at any time point.

In conclusion, prophylaxis with NPD1 attenuated the impairment of general behaviors (buried food test and open field test) and learned behaviors (Y maze test) induced by surgery/anesthesia of aged mice in a fluctuating way.

## **NPD1 modulates the expression of inflammatory cytokines after surgery both in periphery and in CNS**

To assess the effects of NPD1 on the systemic inflammation and neuroinflammation, we firstly measured the changes of TNF- $\alpha$ , IL-6 and IL-10 in blood plasma after surgery. Surgery/anesthesia significantly increased the level of TNF- $\alpha$  and IL-6 at 6 and 9 hours after surgery ( $P < 0.05$ , Fig. 2A-B) but did not change the expression of IL-10 (Fig. 2C). Though a single dose of NPD1 did not completely reverse the increase of proinflammatory cytokines to the control condition, it markedly reduced the levels of TNF- $\alpha$  and IL-6 at 6 hours after surgery ( $P < 0.05$ , Fig. 2A-B). Besides, pretreatment of NPD1 increased the expression of IL-10, a crucial cytokine during the resolution phase of inflammation, at 6 hours after surgery ( $P < 0.05$ , Fig. 2C). Secondly, we measured these cytokines in the hippocampus and prefrontal cortex, two key brain regions related to memory network [33, 34]. Surgery/anesthesia induced a marked increase in the expression of TNF- $\alpha$  and IL-6 at 6 and 9 hours after surgery both in the hippocampus and prefrontal cortex compared to the control condition ( $P < 0.05$ , Fig. 2D-E, G-H). Prophylaxis NPD1 significantly decreased the expression of TNF- $\alpha$  and IL-6 at 6 and 9 h compared to the Surgery group in these brain regions ( $P < 0.05$ , Fig. 2D-E, G-H). Notably, pretreatment with NPD1 increased the expression of IL-10 not only in the hippocampus at 6 and 9 hours after surgery ( $P < 0.05$ , Fig. 2F), but also in the prefrontal cortex at 6 h after surgery ( $P < 0.05$ , Fig. 2L). No effects on these cytokines were reported when treated with NPD1 alone.

## **NPD1 prophylaxis alleviates the leakage of BBB induced by surgery/anesthesia**

The breakdown of blood-brain barrier (BBB) has been reported to be associated with delirium and perioperative neurocognitive disorders [35, 36], herein we employed a well-established dye injection assay

to investigate the integrity of BBB [28, 29] under the treatment of surgery/anesthesia with or without NPD1.

The immunofluorescence images revealed that 10-kDa dextran was primarily confined to vessels in the Control group, NPD1 group and NPD1 + Surgery group. By contrast, the signal of dextran were detected in the brain parenchyma around vessels in the Surgery group (Fig. 3A). To quantitate the extravascular dextran, spectrophotometric quantification of 10-kDa dextran-Texas Red from brain tissue extracts was performed. Both in the hippocampus and prefrontal cortex, we found that surgery/anesthesia increased the level of extravascular 10-kDa dextran as compared to the control condition, while NPD1 prophylaxis decreased the leakage of dextran induced by surgery/anesthesia ( $P < 0.05$ , Fig. 3B-C).

We next examined the effects of NPD1 on the expression of occludin, claudin-5 and ZO-1 after surgery, which are the tight junction (TJ) associated proteins to maintain the integrity of BBB [37, 38]. By quantitative western blot we found that there was a marked decrease in the expression of ZO-1, claudin-5 and occludin both in the hippocampus and prefrontal cortex at 24 hours after surgery, while pretreatment with NPD1 significantly attenuated the reduction of these proteins ( $P < 0.05$ , Fig. 4C-H). Preemptive administration of NPD1 alone did not change the homeostasis of BBB.

## **NPD1 reverses the reactive states of astrocytes and microglia in the hippocampus and prefrontal cortex**

We measured the changes of immunoreactivity of GFAP and Iba-1 in the hippocampus and prefrontal cortex to assess the reactive states of microglia and astrocyte, which represent the major pathological manifestation of neuroinflammation [39–42]. Astrocytes in the hippocampus and prefrontal cortex showed significant morphological changes with shorter and de-ramified processes, atrophic cell soma and reduced GFAP immunoreactive area after surgery compared to the control condition ( $P < 0.05$ , Fig. 5A, B, D). By contrast, mice underwent surgery but pretreated with NPD1 retained the stellate shape of classical astrocytes, with longer processes and similar immunoreactive area to the Control group ( $P < 0.05$ , Fig. 5A, B, D).

NPD1 also attenuated microglial activation as measured by changes in the expression of Iba-1. Surgery induced the amoeba-like morphology of microglia and increased Iba-1 immunoreactive area in the hippocampus and prefrontal cortex compared with the control condition ( $P < 0.05$ , Fig. 5A, C, E), while preemptive administration of NPD1 significantly restored the ramified shape of microglia and reduced cellular area ( $P < 0.05$ , Fig. 5A, C, E). There were neither significant changes in GFAP nor Iba-1 were observed in the NPD1 group.

## **NPD1 alleviates the expression level of pro-inflammatory cytokine and promotes the macrophage polarization toward**

## M2 in the LPS-stimulated BMDMs

NPD1 has been reported to exert proresolving effect by immunoregulation, including blocking neutrophil infiltration and promoting phagocytosis *in vivo* [19, 43], which process is related with the reaction of polarized macrophages [44, 45]. Herein we assessed the effect of NPD1 on LPS-stimulated BMDMs by testing the specific cell markers of polarized macrophages, and the expression of inflammatory cytokines. After identified the particular macrophage marker CD68 in primary BMDMs (Fig. 6A), we stimulated BMDMs with LPS, with or without NPD1 for 24 hours. The polarization of BMDMs were analyzed through the expression of M1 marker CD16/CD32 and M2 marker CD206 (Fig. 6B-C). Quantitative analysis of flow cytometry showed that the population of M1 was significantly increased in the LPS group compared to the Control group ( $P < 0.05$ , Fig. 6D). NPD1 co-incubation tend to downregulate the macrophage polarization to M1, and markedly increased the population of M2 as compared to incubated with LPS alone ( $P < 0.01$ , Fig. 6D-E). The levels of TNF- $\alpha$  and IL-12 was significantly increased by LPS stimulation ( $P < 0.05$ , Fig. 6F, H), while co-incubation with NPD1 decreased the expression of these two cytokines ( $P < 0.05$ , Fig. 6F, H). Incubation with LPS alone increased the level of IL-10 compared to control condition ( $P < 0.05$ , Fig. 6G), suggesting the there were spontaneous initiation of resolution in the inflammation, but co-cultured with NPD1 elevated the expression of IL-10 in further ( $P < 0.05$ , Fig. 6G).

## Discussion

In the present study, we demonstrate that NPD1, a novel lipid derived mediator of SPMs, contributes to the postoperative recovery of POD-like behavior in aged mice by its anti-inflammatory and proresolving effect. Our results indicate that prophylaxis with NPD1 at peripheral injured site alleviates systemic inflammatory response and protects BBB integrity after laparotomy. What's more, it limits neuroinflammation both in the hippocampus and prefrontal cortex, according to the expression of inflammatory cytokines and reactive states of microglia and astroglia in these brain regions. These protective actions against inflammation displayed by NPD1 may relate to macrophage polarization toward M2, as we showed in the *in vitro* experiment. To the best of our knowledge, this is the first report of the effects of NPD1 in a rodent model of POD.

Accumulative evidence has identified the pivotal role of neuroinflammation in the occurrence of POD, while peripheral inflammation is considered to be the initiation of neuroinflammation [36, 46, 47]. In the aseptic surgery setting, injured cells activate BMDMs by releasing damage-associated molecular patterns (DAMPs) that bind to Toll-like receptors (TLRs) of BMDMs, accordingly upregulating the expression of pro-inflammatory cytokines such as TNF- $\alpha$ , IL-1 $\beta$  and IL-6 [48–50]. These cytokines can cause further activation of DAMPs in positive feedback, eventually leads to the augment of inflammation [47, 51]. Our results demonstrate that NPD1 attenuates the systemic release of TNF- $\alpha$  and IL-6 after surgery, which are the pivotal cytokines to appear after trauma [47]. These findings are consistent with the potent anti-inflammatory activity of NPD1 in many other disease models that associated with inflammation, for instance, peritonitis [52], corneal damage [53], asthma [54], and inflammatory pain [55]. In a peritonitis model of murine, PD1/NPD1 has been proven to effectively attenuate polymorphonuclear neutrophil

infiltration and the expression of pro-inflammatory cytokines even at a very small dose (1 ng/mouse) [19, 52, 56]. Furthermore, preemptive administration with NPD1 increases the systemic expression of IL-10, one of the most important mediators in the inflammatory resolution as a potent suppressor to classical macrophage activation [57]. It has been demonstrated that inflammatory cytokines, such as TNF- $\alpha$ , IL-6, IL-1 $\beta$ , and IL-12, are strictly relevant to M1-like macrophages, while IL-10 is primarily secreted by M2-like macrophages [25, 44]. The changes of cytokine profile in the periphery suggest that the macrophage polarization toward M2 may be linked with NPD1.

The breakdown of BBB is seen as a hallmark of neuroinflammation, because this disruption facilitates the infiltration of peripheral immunocompetent cells and cytokines to the immunologically privileged brain [58–60]. The barrier function of BBB is mainly created by the tight junctions of brain microvascular endothelial cells [61]. TNF- $\alpha$  and IL-6 have been reported to disturb the integrity of BBB by reducing the expression of TJ associated proteins between neurovascular endothelium [62, 63]. Notably, TNF- $\alpha$  can upregulate cyclooxygenase 2 isozyme (COX2) in brain microvascular endothelium, thereby increase the local generation of prostaglandins, which has a potent ability to increase vascular permeability [64, 65]. NPD1, as well as its precursor DHA, has shown protective activity for BBB and neurocognitive behavior after experimental ischemic stroke [66, 67], which was also noted in our model. The restoration of impaired BBB by preemptive NPD1 administration may be indirect, attributing to the modulated profile of cytokines in circulation we discussed above, as the same mechanism of how NPD1 alleviated leakage in the laser induced choroidal neovascularization [68]. Interestingly, synthesis of PDs is an enzymatic process via lipoxygenase (LOX) mechanism, while the transcription of LOX is launched by the same signaling pathways for producing prostaglandin E2 and D2 [65, 69]. The production of IL-10 also requires the participation of prostaglandins [57]. This kind of temporal-spatial interaction between inflammatory mediators can explain, at least in part, why there is no valid evidence for inflammatory inhibitors to treat POD or other neurocognitive disorders, for they may hinder the resolution phase of inflammation. Therefore, NPD1, as well as other SPMs, may be desirable therapies for the inflammation-driven diseases.

In addition to mitigate peripheral inflammatory response, NPD1 subsides the activation of glia cells and the expression of inflammatory cytokines in the hippocampus and prefrontal cortex. As resident macrophages in CNS, microglia act as immune surveillance and respond to different kinds of pathological stimuli [70]. Once activated, microglia rapidly switch to a pro-inflammatory phenotype with stout morphology, and enhance the production of pro-inflammatory molecules such as IL-1 $\alpha$ , TNF- $\alpha$  and complement component 1q (C1q) [71, 72]. These specific cytokines along with cell debris released by classically activated microglia can trigger the transformation of astroglia to A1, the detrimental reactive phenotype of astrocytes [39, 40, 72, 73]. A1 astrocytes lose the supportive abilities in CNS, *i.e.* maintaining synaptic functions and phagocytic capacity, and secretes neurotoxin to induce neuronal death at meanwhile [72, 74]. In our model of POD, NPD1 reverts the morphological changes of microglia and astrocytes both in the hippocampus and prefrontal cortex to their original forms, representing the restorative transformation from the inflamed phenotype to their resting states, and thus modified the pro-inflammatory milieu by modulating the secretion of inflammatory cytokines. It is thus not surprising that NPD1 pretreatment facilitates the recovery of POD-like behavior in aged mice, for these two beneficiary

brain regions act in concert to shape emotion, learn and organize memory, and transform information [75, 76]. Though microglia share similar properties with peripheral macrophages, it may not be the target cell that is affected by NPD1. Recently, parkin-associated endothelin-like receptor (Pael-R), also known as GPR37, has been identified to be the particular receptor for NPD1 [55]. GPR37 is enriched in oligodendrocytes and astrocytes, but not microglia [55, 77]. In this context, the anti-inflammatory and proresolving effects of NPD1 in CNS may harness through different cell types, and the underlying mechanism needs further investigation.

BMDMs have been shown to be the bridge to link the peripheral and central immune systems since they can infiltrate into the brain in conditions characterized by neuroinflammation [78, 79]. Their function can be deleterious or favorable, depending on their polarization states to extracellular milieu [25, 80]. Other members of SPMs that derived from the same precursor with NPD1 have been shown to induce the M2 polarization [81–83], which suggest the similar property maybe exist in NPD1. The phenotypic skewing of inflammatory mediators *in vitro* has been also promoted by NPD1, that is, attenuating the M1 macrophage markers (TNF- $\alpha$  and IL-12) and elevating the M2 macrophage marker (IL-10). Also, the shift of specific cell receptors on LPS-stimulated BMDMs from M1 to M2 has verified the M2 polarization is induced by NPD1 in further. These findings, along with those of *in vivo* in the present research, suggest that the proresolving effect of NPD1 may be linked to transformation in macrophage polarization to the M2 phenotype. However, three subsets of M2 phenotype, named as M2a, M2b, and M2c, each of which has different protective properties, have been identified among the M2 phenotype [84]. It is thus essential to explore the exhaustive effect of NPD1 on macrophages and inflammation in further.

There are several limitations to our research. Firstly, we only assessed the cellular constituents in CNS and morphological changes of glia cells, but not the influence of the interventions for neurons. The glia-neuron crosstalk, especially in the hippocampus, is highly involved in the normal function of neurons to form memory and consciousness [42, 85, 86]. Besides, a recent study has described the analgesic effect of NPD1 [55]. Though we used local analgesics to prevent postoperative pain, it is difficult to determine whether NPD1 enhanced the postoperative recovery of mice by acting in an additive fashion with local analgesics to relieve the pain. Secondly, we only focused on the impact of NPD1 in regulating inflammation in our study, but not the signaling pathways leading to the phenomenon. It has been documented that the neuroprotection of NPD1 is elicited through NF- $\kappa$ B or PI3K/Akt phosphorylation signaling [22, 87–89], which gives the reference to illuminate the particular pathways of NPD1 in the perioperative setting.

## Conclusion

The present study identifies the novel role of NPD1 in regulating postoperative inflammation not only in periphery but also in the hippocampus and prefrontal cortex, which results in relieving the ensuing POD-like behavior of mice. These protective effects of NPD1 is related to its modulation of macrophage polarization. Collectively, these findings indicate the potential of NPD1 to be a novel therapy for neuroinflammation and POD.

## Abbreviations

POD: Postoperative delirium; SPMs:Specialized proresolving lipid mediators; TJ:Tight junction; BMDMs:Bone marrow-derived macrophages; TNF- $\alpha$ :Tumor necrosis factor- $\alpha$ ; IL-6:Interleukin-6; BBB:Blood-brain barrier; CNS:Central nervous system; PD:Protectin D; NPD1:Neuroprotectin D1; DHA:Omega-3-polyunsaturated fatty acid docosahexaenoic acid; PBS:phosphate-buffered saline; ; GFAP:Glial fibrillary acidic protein; IBA-1:Ionized calcium-binding adaptor molecule 1; SEM:Standard error of the mean

## Declarations

## Availability of data and materials

All data will be made available from the corresponding author, with a reasonable request.

## Ethics approval

The experimental protocol was approved by the Animal Ethics Committee of Zhongnan Hospital of Wuhan University, Hubei, China, and all experiments were performed in accordance with the National Institutes of Health Guidelines for the Care and Use of Laboratory Animals.

## Consent for publication

Not applicable.

## Competing interests

The authors declare no conflict of interest.

## Funding

This research was supported by the National Natural Science Foundation of China (no. 81371195 and no. 81870851), and a research grant from the Outstanding Talented Young Doctor Program of Hubei Province (2019).

## Author contributions

YZ designed and performed the experiment, collected and analyzed the data, and prepared the manuscript. JW and XL were involved in preparing the animal models and participated in interpreting the

results. KL contributed to behavioral testing. LC was involved in biochemical analysis. YZ and JW participated in the statistical analysis. MP contributed to the study concept and design, secured funding for the project, and prepared and critically revised the manuscript. All authors reviewed the manuscript.

## Acknowledgements

Not applicable.

## References

1. Inouye SK, Westendorp RGJ, Saczynski JS. Delirium in elderly people. *Lancet*. 2014;383:911–22.
2. Robinson TN, Eiseman B. Postoperative delirium in the elderly: diagnosis and management. *Clin Interv Aging*. 2008;3:351–5.
3. Partridge L, Deelen J, Slagboom PE. Facing up to the global challenges of ageing. *Nature*. 2018;561:45–56.
4. Marcantonio ER. Delirium. *Annals of Internal Medicine* 2011, 154:ITC6-1.
5. Bruce AJ, Ritchie CW, Blizzard R, Lai R, Raven P. The incidence of delirium associated with orthopedic surgery: a meta-analytic review. *Int Psychogeriatr*. 2006;19:197–214.
6. American Geriatrics Society Expert Panel on Postoperative Delirium in Older A. Postoperative delirium in older adults: best practice statement from the American Geriatrics Society. *J Am Coll Surg*. 2015;220:136–48 e131.
7. Hirsch J, Vacas S, Terrando N, Yuan M, Sands LP, Kramer J, Bozic K, Maze MM, Leung JM. Perioperative cerebrospinal fluid and plasma inflammatory markers after orthopedic surgery. *J Neuroinflamm*. 2016;13:211–1.
8. Maclullich AMJ, Ferguson KJ, Miller T, de Rooij SEJA, Cunningham C. Unravelling the pathophysiology of delirium: a focus on the role of aberrant stress responses. *J Psychosom Res*. 2008;65:229–38.
9. Terrando N, Eriksson LI, Ryu JK, Yang T, Monaco C, Feldmann M, Jonsson Fagerlund M, Charo IF, Akassoglou K, Maze M. Resolving postoperative neuroinflammation and cognitive decline. *Ann Neurol*. 2011;70:986–95.
10. Hu J, Feng X, Valdearcos M, Lutrin D, Uchida Y, Koliwad SK, Maze M. Interleukin-6 is both necessary and sufficient to produce perioperative neurocognitive disorder in mice. *Br J Anaesth*. 2018;120:537–45.
11. Prinz M, Priller J. Microglia and brain macrophages in the molecular age: from origin to neuropsychiatric disease. *Nat Rev Neurosci*. 2014;15:300–12.
12. Girard S, Brough D, Lopez-Castejon G, Giles J, Rothwell NJ, Allan SM. Microglia and macrophages differentially modulate cell death after brain injury caused by oxygen-glucose deprivation in organotypic brain slices. *Glia*. 2013;61:813–24.

13. Simard AR, Soulet D, Gowing G, Julien J-P, Rivest S. Bone Marrow-Derived Microglia Play a Critical Role in Restricting Senile Plaque Formation in Alzheimer's Disease. *Neuron*. 2006;49:489–502.
14. Perry VH, Teeling J. Microglia and macrophages of the central nervous system: the contribution of microglia priming and systemic inflammation to chronic neurodegeneration. *Semin Immunopathol*. 2013;35:601–12.
15. D'Mello C, Le T, Swain MG. Cerebral microglia recruit monocytes into the brain in response to tumor necrosis factor- $\alpha$  signaling during peripheral organ inflammation. *The Journal of neuroscience: the official journal of the Society for Neuroscience*. 2009;29:2089–102.
16. Plaschke K, Weigand MA, Fricke F, Kopitz J. Neuroinflammation: effect of surgical stress compared to anaesthesia and effect of physostigmine. *Neurol Res*. 2016;38:397–405.
17. Skvarc DR, Berk M, Byrne LK, Dean OM, Dodd S, Lewis M, Marriott A, Moore EM, Morris G, Page RS, Gray L. Post-Operative Cognitive Dysfunction: An exploration of the inflammatory hypothesis and novel therapies. *Neuroscience Biobehavioral Reviews*. 2018;84:116–33.
18. Serhan CN, Chiang N, Dalli J, Levy BD. Lipid mediators in the resolution of inflammation. *Cold Spring Harb Perspect Biol*. 2014;7:a016311–1.
19. Hong S, Gronert K, Devchand PR, Moussignac R-L, Serhan CN. Novel Docosatrienes and 17S-Resolvins Generated from Docosahexaenoic Acid in Murine Brain, Human Blood, and Glial Cells: AUTACOIDS IN ANTI-INFLAMMATION. *J Biol Chem*. 2003;278:14677–87.
20. Serhan CN, Hong S, Gronert K, Colgan SP, Devchand PR, Mirick G, Moussignac R-L. Resolvins: a family of bioactive products of omega-3 fatty acid transformation circuits initiated by aspirin treatment that counter proinflammation signals. *The Journal of experimental medicine*. 2002;196:1025–37.
21. Hong S, Tian H, Lu Y, Laborde JM, Muhale FA, Wang Q, Alapure BV, Serhan CN, Bazan NG. Neuroprotectin/protectin D1: endogenous biosynthesis and actions on diabetic macrophages in promoting wound healing and innervation impaired by diabetes. *Am J Physiol Cell Physiol*. 2014;307:C1058–67.
22. Mukherjee PK, Marcheselli VL, Serhan CN, Bazan NG. Neuroprotectin D1: a docosahexaenoic acid-derived docosatriene protects human retinal pigment epithelial cells from oxidative stress. *Proc Natl Acad Sci USA*. 2004;101:8491–6.
23. Lukiw WJ, Cui J-G, Marcheselli VL, Bodker M, Botkjaer A, Gotlinger K, Serhan CN, Bazan NG. A role for docosahexaenoic acid-derived neuroprotectin D1 in neural cell survival and Alzheimer disease. *J Clin Invest*. 2005;115:2774–83.
24. Safavynia SA, Goldstein PA. The Role of Neuroinflammation in Postoperative Cognitive Dysfunction: Moving From Hypothesis to Treatment. *Frontiers in psychiatry*. 2019;9:752–2.
25. Murray P. Macrophage Polarization. *Annual review of physiology* 2016, 79.
26. Peng M, Zhang C, Dong Y, Zhang Y, Nakazawa H, Kaneki M, Zheng H, Shen Y, Marcantonio ER, Xie Z. Battery of behavioral tests in mice to study postoperative delirium. *Sci Rep*. 2016;6:29874.

27. Lu Y, Chen L, Ye J, Chen C, Zhou Y, Li K, Zhang Z, Peng M. Surgery/Anesthesia disturbs mitochondrial fission/fusion dynamics in the brain of aged mice with postoperative delirium. *Aging*. 2020;12:844–65.
28. Ben-Zvi A, Lacoste B, Kur E, Andreone BJ, Mayshar Y, Yan H, Gu C. Mfsd2a is critical for the formation and function of the blood–brain barrier. *Nature*. 2014;509:507–11.
29. Yang S, Gu C, Mandeville ET, Dong Y, Esposito E, Zhang Y, Yang G, Shen Y, Fu X, Lo EH, Xie Z. Anesthesia and Surgery Impair Blood-Brain Barrier and Cognitive Function in Mice. *Front Immunol*. 2017;8:902.
30. Yang M, Crawley JN. Simple behavioral assessment of mouse olfaction. *Curr Protoc Neurosci* 2009, Chap. 8:Unit 8 24.
31. Gould TD, Dao DT, Kovacsics CE. The Open Field Test. 2009;42:1–20.
32. Wheelan N, Webster SP, Kenyon CJ, Caughey S, Walker BR, Holmes MC, Seckl JR, Yau JLW. Short-term inhibition of 11 $\beta$ -hydroxysteroid dehydrogenase type 1 reversibly improves spatial memory but persistently impairs contextual fear memory in aged mice. *Neuropharmacology*. 2015;91:71–6.
33. Place R, Farovik A, Brockmann M, Eichenbaum H. Bidirectional prefrontal-hippocampal interactions support context-guided memory. *Nature neuroscience*. 2016;19:992–4.
34. Preston AR, Eichenbaum H. Interplay of hippocampus and prefrontal cortex in memory. *Current biology: CB*. 2013;23:R764–73.
35. Maldonado JR. Pathoetiological Model of Delirium: a Comprehensive Understanding of the Neurobiology of Delirium and an Evidence-Based Approach to Prevention and Treatment. *Crit Care Clin*. 2008;24:789–856.
36. Subramaniam S, Terrando N. Neuroinflammation and Perioperative Neurocognitive Disorders. *Anesth Analg*. 2019;128:781–8.
37. Luissint A-C, Artus C, Glacial F, Ganeshamoorthy K, Couraud P-O. Tight junctions at the blood brain barrier: physiological architecture and disease-associated dysregulation. *Fluids barriers of the CNS*. 2012;9:23–3.
38. Jiao H, Wang Z, Liu Y, Wang P, Xue Y. Specific Role of Tight Junction Proteins Claudin-5, Occludin, and ZO-1 of the Blood–Brain Barrier in a Focal Cerebral Ischemic Insult. *J Mol Neurosci*. 2011;44:130–9.
39. Joshi AU, Minhas PS, Liddelow SA, Haileselassie B, Andreasson KI, Dorn GW 2nd, Mochly-Rosen D. Fragmented mitochondria released from microglia trigger A1 astrocytic response and propagate inflammatory neurodegeneration. *Nature neuroscience*. 2019;22:1635–48.
40. Norden DM, Trojanowski PJ, Villanueva E, Navarro E, Godbout JP. Sequential activation of microglia and astrocyte cytokine expression precedes increased Iba-1 or GFAP immunoreactivity following systemic immune challenge. *Glia*. 2016;64:300–16.
41. Yang T, Xu G, Newton PT, Chagin AS, Mkrтчian S, Carlstrom M, Zhang XM, Harris RA, Cooter M, Berger M, et al. Maresin 1 attenuates neuroinflammation in a mouse model of perioperative neurocognitive disorders. *Br J Anaesth*. 2019;122:350–60.

42. Terrando N, Gomez-Galan M, Yang T, Carlstrom M, Gustavsson D, Harding RE, Lindskog M, Eriksson LI. Aspirin-triggered resolvin D1 prevents surgery-induced cognitive decline. *FASEB J*. 2013;27:3564–71.
43. Ariel A, Serhan CN. Resolvins and protectins in the termination program of acute inflammation. *Trends Immunol*. 2007;28:176–83.
44. Mosser DM, Edwards JP. Exploring the full spectrum of macrophage activation. *Nat Rev Immunol*. 2008;8:958–69.
45. Tabas I. Macrophage death and defective inflammation resolution in atherosclerosis. *Nature reviews Immunology*. 2010;10:36–46.
46. Groh J, Martini R. Neuroinflammation as modifier of genetically caused neurological disorders of the central nervous system: Understanding pathogenesis and chances for treatment. *Glia*. 2017;65:1407–22.
47. Terrando N, Monaco C, Ma D, Foxwell BMJ, Feldmann M, Maze M. Tumor necrosis factor-alpha triggers a cytokine cascade yielding postoperative cognitive decline. *Proc Natl Acad Sci USA*. 2010;107:20518–22.
48. Akira S, Takeda K. Toll-like receptor signalling. *Nat Rev Immunol*. 2004;4:499–511.
49. Zhang Q, Raoof M, Chen Y, Sumi Y, Sursal T, Junger W, Brohi K, Itagaki K, Hauser CJ. Circulating mitochondrial DAMPs cause inflammatory responses to injury. *Nature*. 2010;464:104–7.
50. Lotze MT, Tracey KJ. High-mobility group box 1 protein (HMGB1): nuclear weapon in the immune arsenal. *Nat Rev Immunol*. 2005;5:331–42.
51. Gabay C, Lamacchia C, Palmer G. IL-1 pathways in inflammation and human diseases. *Nature reviews Rheumatology*. 2010;6:232–41.
52. Ariel A, Fredman G, Sun Y-P, Kantarci A, Van Dyke TE, Luster AD, Serhan CN. Apoptotic neutrophils and T cells sequester chemokines during immune response resolution through modulation of CCR5 expression. *Nature immunology*. 2006;7:1209–16.
53. Gronert K, Maheshwari N, Khan N, Hassan I, Dunn M, Schwartzman M. A Role for the Mouse 12/15-Lipoxygenase Pathway in Promoting Epithelial Wound Healing and Host Defense. *J Biol Chem*. 2005;280:15267–78.
54. Levy BD, Kohli P, Gotlinger K, Haworth O, Hong S, Kazani S, Israel E, Haley KJ, Serhan CN: Protectin D1 is generated in asthma and dampens airway inflammation and hyperresponsiveness. *Journal of immunology (Baltimore, Md: 1950)* 2007, 178:496–502.
55. Bang S, Xie Y-K, Zhang Z-J, Wang Z, Xu Z-Z, Ji R-R. GPR37 regulates macrophage phagocytosis and resolution of inflammatory pain. *J Clin Investig*. 2018;128:3568–82.
56. Ariel A, Li PL, Wang W, Tang WX, Fredman G, Hong S, Gotlinger KH, Serhan CN. The docosatriene protectin D1 is produced by TH2 skewing and promotes human T cell apoptosis via lipid raft clustering. *J Biol Chem*. 2005;280:43079–86.

57. Mosser DM, Zhang X. Interleukin-10: new perspectives on an old cytokine. *Immunological reviews*. 2008;226:205–18.
58. Galea I, Bechmann I, Perry VH. What is immune privilege (not)? *Trends Immunol*. 2007;28:12–8.
59. He H-J, Wang Y, Le Y, Duan K-M, Yan X-B, Liao Q, Liao Y, Tong J-B, Terrando N, Ouyang W. Surgery upregulates high mobility group box-1 and disrupts the blood-brain barrier causing cognitive dysfunction in aged rats. *CNS Neurosci Ther*. 2012;18:994–1002.
60. Palmela I, Brites D, Brito M. Blood-brain barrier in health and disease. *The Blood-Brain Barrier: New Research* 2012:201–218.
61. Pardridge WM. The blood-brain barrier: bottleneck in brain drug development. *NeuroRx: the journal of the American Society for Experimental NeuroTherapeutics*. 2005;2:3–14.
62. Rochfort K, Collins L, McLoughlin A, Cummins P. TNF- $\alpha$ -mediated disruption of cerebrovascular endothelial barrier integrity in vitro involves the production of proinflammatory IL-6. *Journal of neurochemistry* 2015.
63. Blecharz-Lang K, Wagner J, Fries A, Nieminen-Kelhä M, Rösner J, Schneider U, Vajkoczy P. Interleukin 6-Mediated Endothelial Barrier Disturbances Can Be Attenuated by Blockade of the IL6 Receptor Expressed in Brain Microvascular Endothelial Cells. *Translational Stroke Research* 2018, 9.
64. Engblom D, Ek M, Saha S, Dahlstrand A, Jakobsson P-J, Blomqvist A. Prostaglandins as inflammatory messengers across the blood-brain barrier. *J Mol Med*. 2002;80:5–15.
65. Rajakariar R, Yaqoob M, Gilroy D. COX-2 In inflammation and resolution. *Mol Interv*. 2006;6:199–207.
66. Belayev L, Hong S-H, Menghani H, Marcell SJ, Obenaus A, Freitas RS, Khoutorova L, Balaszczuk V, Jun B, Oriá RB, Bazan NG. Docosanoids Promote Neurogenesis and Angiogenesis, Blood-Brain Barrier Integrity, Penumbra Protection, and Neurobehavioral Recovery After Experimental Ischemic Stroke. *Mol Neurobiol*. 2018;55:7090–106.
67. Belayev L, Khoutorova L, Atkins KD, Eady TN, Hong S, Lu Y, Obenaus A, Bazan NG. Docosahexaenoic Acid therapy of experimental ischemic stroke. *Translational stroke research*. 2011;2:33–41.
68. Sheets KG, Zhou Y, Ertel MK, Knott EJ, Regan CE Jr, Elison JR, Gordon WC, Gjorstrup P, Bazan NG. Neuroprotectin D1 attenuates laser-induced choroidal neovascularization in mouse. *Molecular vision*. 2010;16:320–9.
69. Bannenberg G, Chiang N, Ariel A, Arita M, Tjonahen E, Gotlinger K, Hong S, Serhan C: Molecular Circuits of Resolution: Formation and Actions of Resolvins and Protectins. *Journal of immunology (Baltimore, Md: 1950)* 2005, 174:4345–4355.
70. Kettenmann H, Kirchhoff F, Verkhratsky A. Microglia: New Roles for the Synaptic Stripper. *Neuron*. 2013;77:10–8.
71. Clausen BH, Lambertsen KL, Babcock AA, Holm TH, Dagnaes-Hansen F, Finsen B. Interleukin-1 $\beta$  and tumor necrosis factor- $\alpha$  are expressed by different subsets of microglia and macrophages after ischemic stroke in mice. *J Neuroinflamm*. 2008;5:46–6.

72. Liddelow SA, Guttenplan KA, Clarke LE, Bennett FC, Bohlen CJ, Schirmer L, Bennett ML, Münch AE, Chung W-S, Peterson TC, et al. Neurotoxic reactive astrocytes are induced by activated microglia. *Nature*. 2017;541:481–7.
73. Zamanian JL, Xu L, Foo LC, Nouri N, Zhou L, Giffard RG, Barres BA. Genomic analysis of reactive astrogliosis. *The Journal of neuroscience: the official journal of the Society for Neuroscience*. 2012;32:6391–410.
74. Gómez-Galán M, Dimitri DB, Van Eeckhaut A, Smolders I, Lindskog M. Dysfunctional astrocytic regulation of glutamate transmission in a rat model of depression. *Molecular psychiatry* 2012, 18.
75. Eichenbaum H. Prefrontal-hippocampal interactions in episodic memory. *Nature reviews Neuroscience* 2017, 18.
76. Tyng CM, Amin HU, Saad MNM, Malik AS. The Influences of Emotion on Learning and Memory. *Frontiers in psychology*. 2017;8:1454–4.
77. Cahoy JD, Emery B, Kaushal A, Foo LC, Zamanian JL, Christopherson KS, Xing Y, Lubischer JL, Krieg PA, Krupenko SA, et al. A transcriptome database for astrocytes, neurons, and oligodendrocytes: a new resource for understanding brain development and function. *The Journal of neuroscience: the official journal of the Society for Neuroscience*. 2008;28:264–78.
78. Tanaka R, Komine-Kobayashi M, Mochizuki H, Yamada M, Furuya T, Migita M, Shimada T, Mizuno Y, Urabe T. Migration of enhanced green fluorescent protein expressing bone marrow-derived microglia/macrophage into the mouse brain following permanent focal ischemia. *Neuroscience*. 2003;117:531–9.
79. Liu Y, Uberti MG, Dou H, Banerjee R, Grotepas CB, Stone DK, Rabinow BE, Gendelman HE, Boska MD. Ingress of blood-borne macrophages across the blood-brain barrier in murine HIV-1 encephalitis. *J Neuroimmunol*. 2008;200:41–52.
80. Italiani P, Boraschi D. From Monocytes to M1/M2 Macrophages: Phenotypical vs. Functional Differentiation *Frontiers in immunology*. 2014;5:514–4.
81. Marcon R, Bento AF, Dutra RC, Bicca MA, Leite DFP, Calixto JB. Maresin 1, a Proresolving Lipid Mediator Derived from Omega-3 Polyunsaturated Fatty Acids, Exerts Protective Actions in Murine Models of Colitis. *J Immunol*. 2013;191:4288.
82. Titos E, Rius B, González-Pérez A, López-Vicario C, Morán-Salvador E, Martínez-Clemente M, Arroyo V, Clària J. Resolvin D1 and Its Precursor Docosahexaenoic Acid Promote Resolution of Adipose Tissue Inflammation by Eliciting Macrophage Polarization toward an M2-Like Phenotype. *J Immunol*. 2011;187:5408.
83. Akagi D, Chen M, Toy R, Chatterjee A, Conte MS. Systemic delivery of proresolving lipid mediators resolvin D2 and maresin 1 attenuates intimal hyperplasia in mice. *FASEB journal: official publication of the Federation of American Societies for Experimental Biology*. 2015;29:2504–13.
84. Biswas SK, Mantovani A. Macrophage plasticity and interaction with lymphocyte subsets: cancer as a paradigm. *Nat Immunol*. 2010;11:889–96.

85. Chung W-S, Welsh CA, Barres BA, Stevens B. Do glia drive synaptic and cognitive impairment in disease? *Nature neuroscience*. 2015;18:1539–45.
86. Santello M, Toni N, Volterra A. Astrocyte function from information processing to cognition and cognitive impairment. *Nature Neuroscience* 2019.
87. Calandria JM, Asatryan A, Balaszczuk V, Knott EJ, Jun BK, Mukherjee PK, Belayev L, Bazan NG. NPD1-mediated stereoselective regulation of BIRC3 expression through cREL is decisive for neural cell survival. *Cell death differentiation*. 2015;22:1363–77.
88. Belayev L, Mukherjee PK, Balaszczuk V, Calandria JM, Obenaus A, Khoutorova L, Hong S-H, Bazan NG. Neuroprotectin D1 upregulates Iduna expression and provides protection in cellular uncompensated oxidative stress and in experimental ischemic stroke. *Cell death differentiation*. 2017;24:1091–9.
89. Halapin NA, Bazan NG. NPD1 Induction of Retinal Pigment Epithelial Cell Survival Involves PI3K/Akt Phosphorylation Signaling. *Neurochem Res*. 2010;35:1944–7.

## Figures

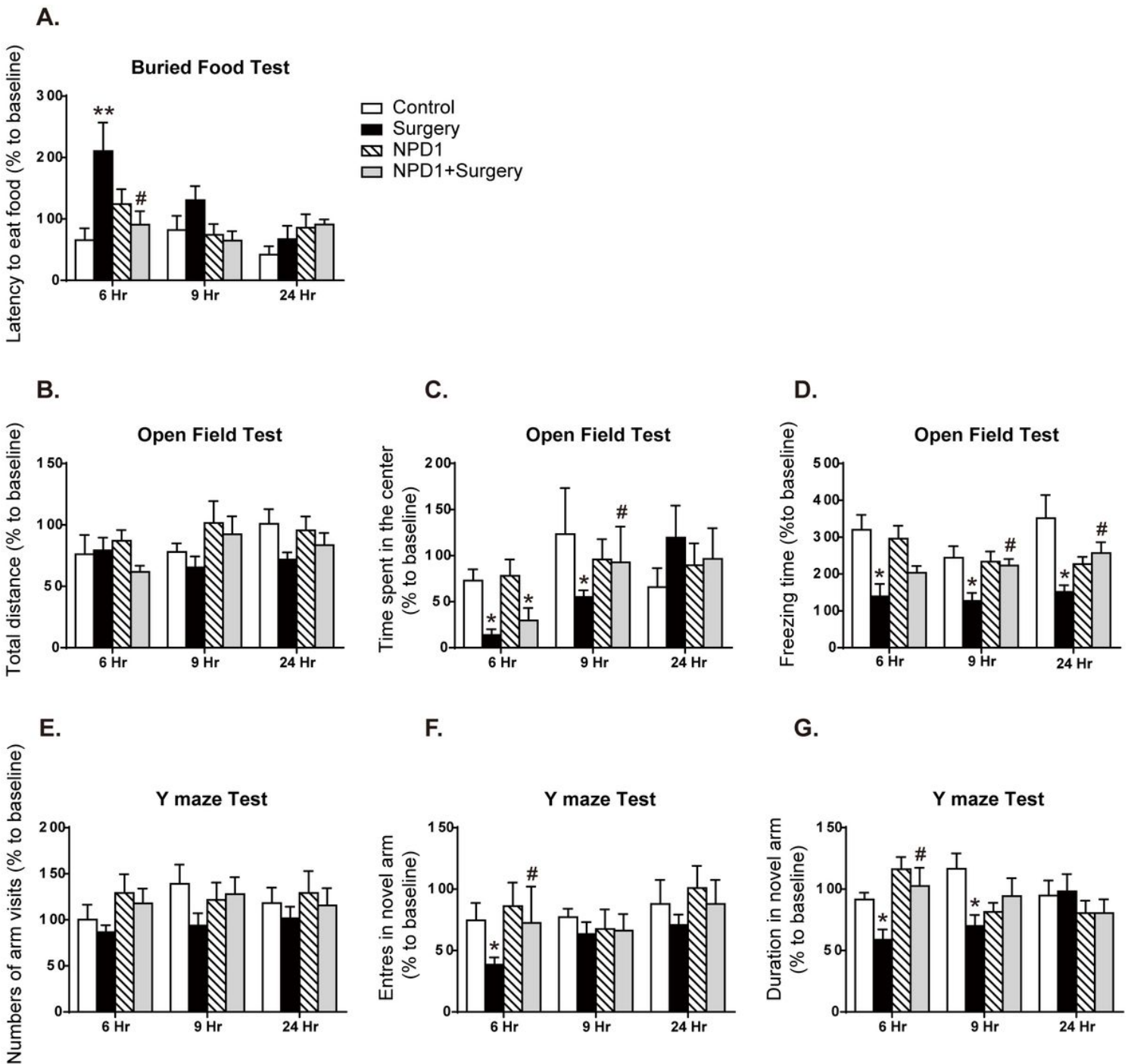


**Figure 1**

Surgery/Anesthesia induces POD-like behavior of aged mice, which can be ameliorated by the preemptive administration of NPD1. At 6, 9, 24 hours after surgery/anesthesia, the buried food test (A), open field test (B-D) and Y maze test (E-G) were executed ordinarily. Data are presented as means  $\pm$  SEM of the mean for each group (n = 8~10 per group). \*P < 0.05 versus the Control group, \*\*P < 0.01 versus the Control group, #P < 0.05 versus the Surgery group.

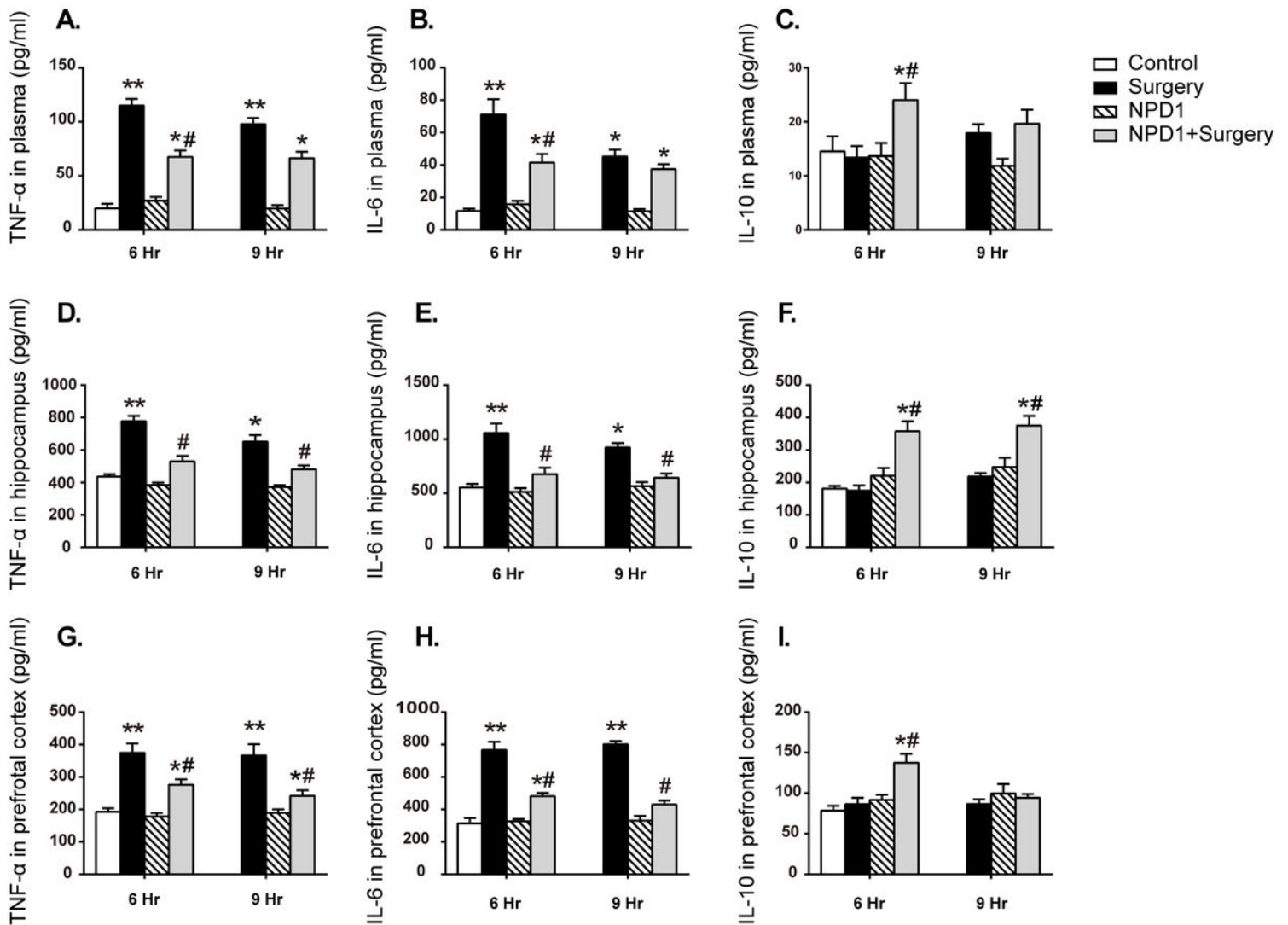


**Figure 2**

Effects of NPD1 on the expression of inflammatory factors in vivo. NPD1 pretreatment alleviated the surgery-induced upregulation of proinflammatory factors and promoted the expression of anti-inflammation factors both in the periphery blood and the central locations such as the hippocampus and prefrontal cortex (B)-(J). NPD1 and these cytokines were measured by ELASA. Data are presented as means  $\pm$  SEM of the mean for each group (n = 4~5 per group). \*P < 0.05 versus the Control group, \*\*P < 0.01 versus the Control group, #P < 0.05 versus the Surgery group.

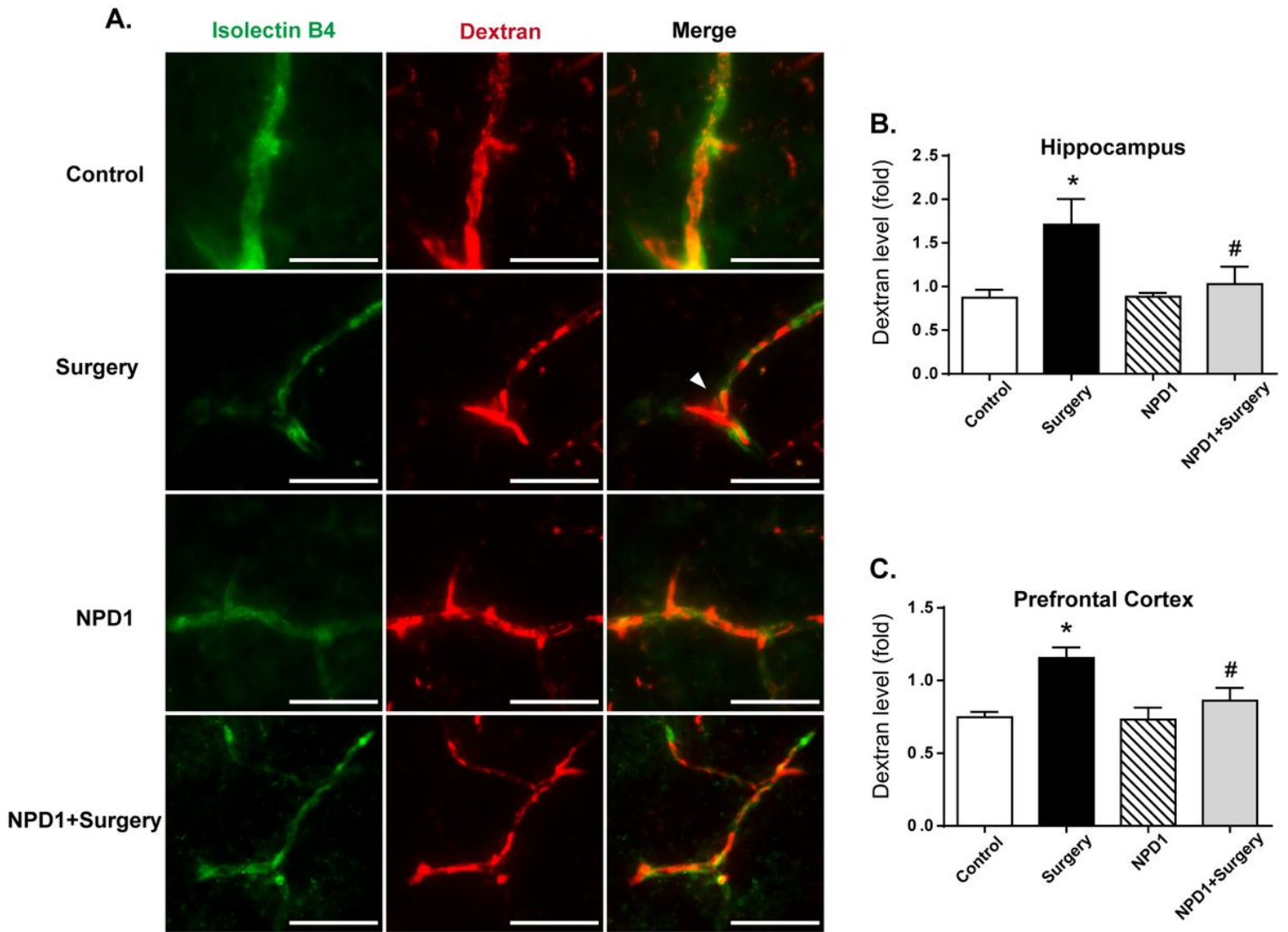


**Figure 3**

NPD1 protects against the leakage of BBB induced by surgery/anesthesia in the hippocampus and prefrontal cortex. Immunostaining of blood vessels (Isolectin B4, green) and intravenous injected dextran (10-kDa, red) in the brain section of the hippocampus at 6 hours after surgery (A). Arrowhead marked area indicated the dextran was extravascular. The spectrophotometric quantification of extravascular dextran (10-kDa) level in the extraction of the hippocampus and prefrontal cortex showed that the surgery/anesthesia increased the permeability of BBB as compared to control, and pretreatment with NPD1 attenuated this phenomenon (B-C). Data are presented as means  $\pm$  SEM of the mean for each group (n = 4~5 per group). \*P < 0.05 versus the Control group, #P < 0.05 versus the Surgery group. Scale bars represent 50  $\mu$ m in (A).

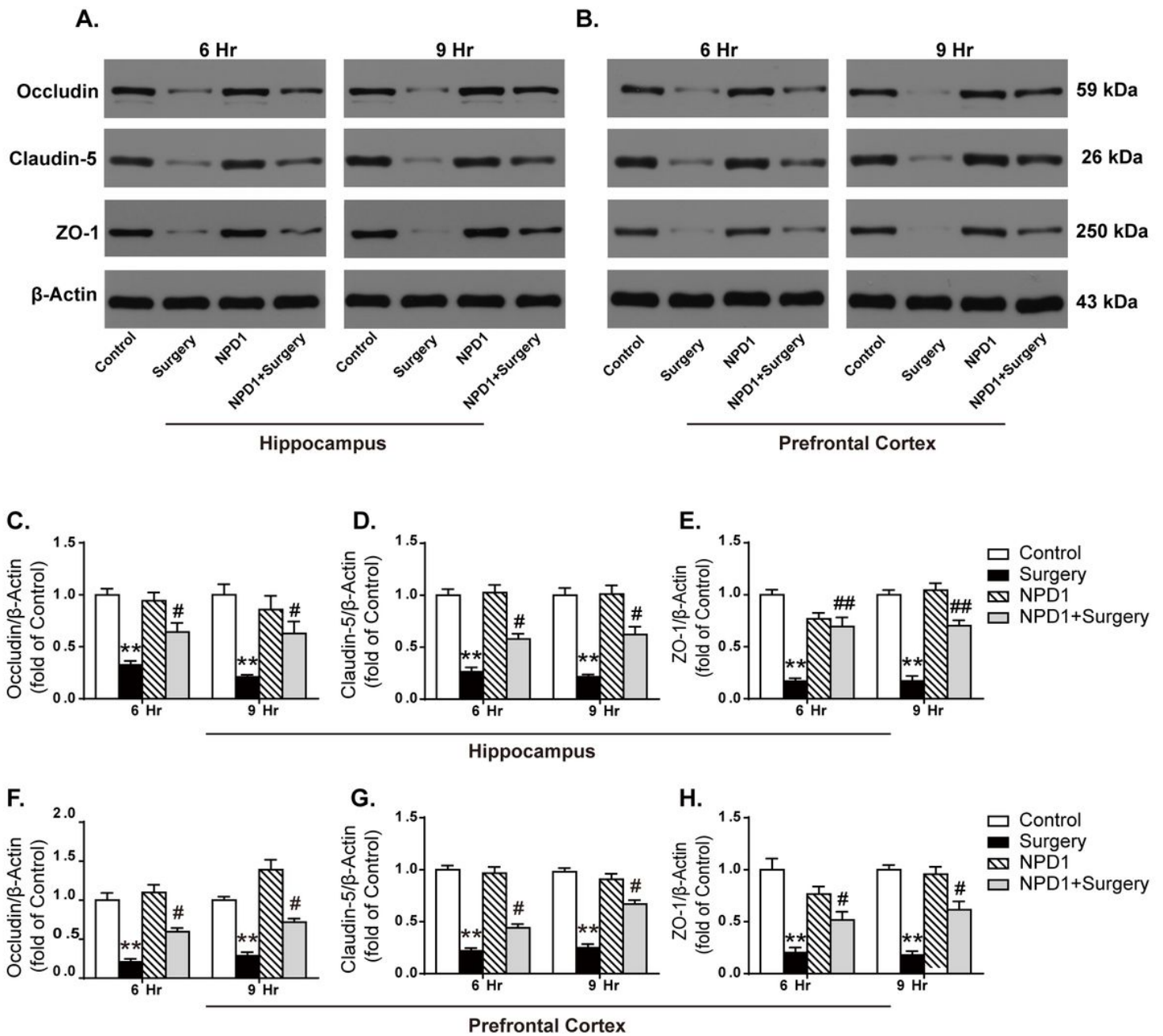


**Figure 4**

NPD1 modulates the expression of TJ associated proteins in the hippocampus and prefrontal cortex after surgery. Representative Western blotting bands of the expression of occludin, claudin-5 and ZO-1 in the hippocampus and prefrontal cortex at 6 and 9 hours after surgery (A, C). Quantification analyses of the expression of occludin, claudin-5 and ZO-1 were normalized to that of  $\beta$ -actin as internal control, and changes in protein levels were presented as folds of those in the Control group (B, D). Data are presented as means  $\pm$  SEM of the mean for each group (n = 4~5 per group). \*\*P < 0.01 versus the Control group, #P < 0.05 versus the Surgery group, ##P < 0.01 versus the Surgery group.

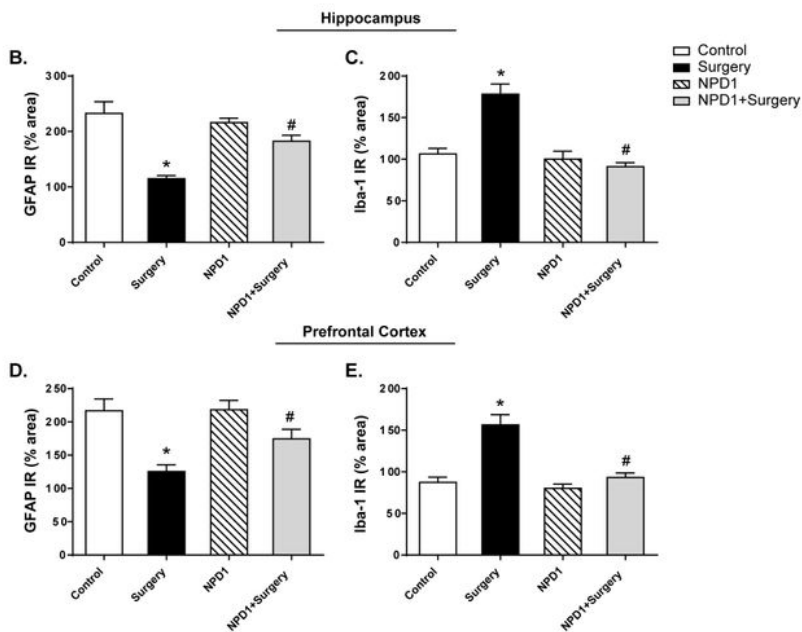
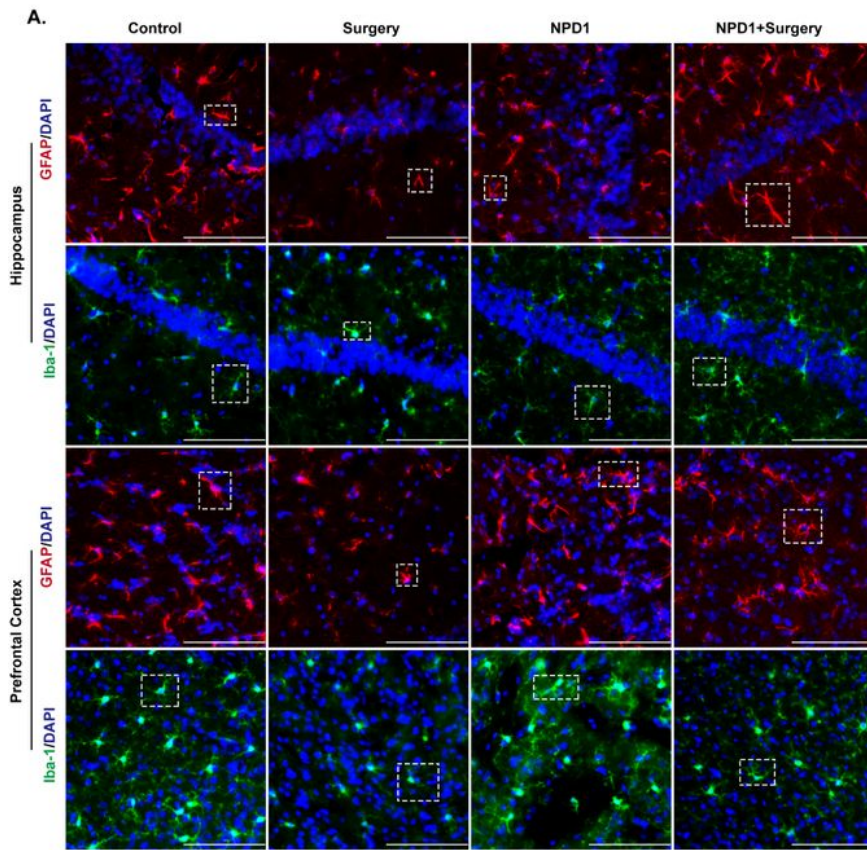


**Figure 5**

NPD1 pretreatment subsides the activation of astrocytes and microglia in the hippocampus and prefrontal cortex that elicited by surgery/anesthesia. Representative images of immunofluorescence showed the expression of GFAP and Iba-1 in the hippocampus and prefrontal cortex at 24 h after surgery (A-B, E-F). Surgery/anesthesia caused distinct changes in the morphology of glial cells with shorter processes and reduced cell soma for astrocytes, and amoeba-like morphology for microglial. Preemptive

administration of NPD1 significantly restored the classic stellate shape of astrocytes and the ramified shape of microglial. Quantification results of the immunostaining at 24 h after surgery showed in (C-D, G-H). Data are presented as means  $\pm$  SEM of the mean for each group (n = 4~5 per group). \*P < 0.05 versus the Control group, #P < 0.05 versus the Surgery group. Scale bars represent 100  $\mu$ m in (A-B and E-F).

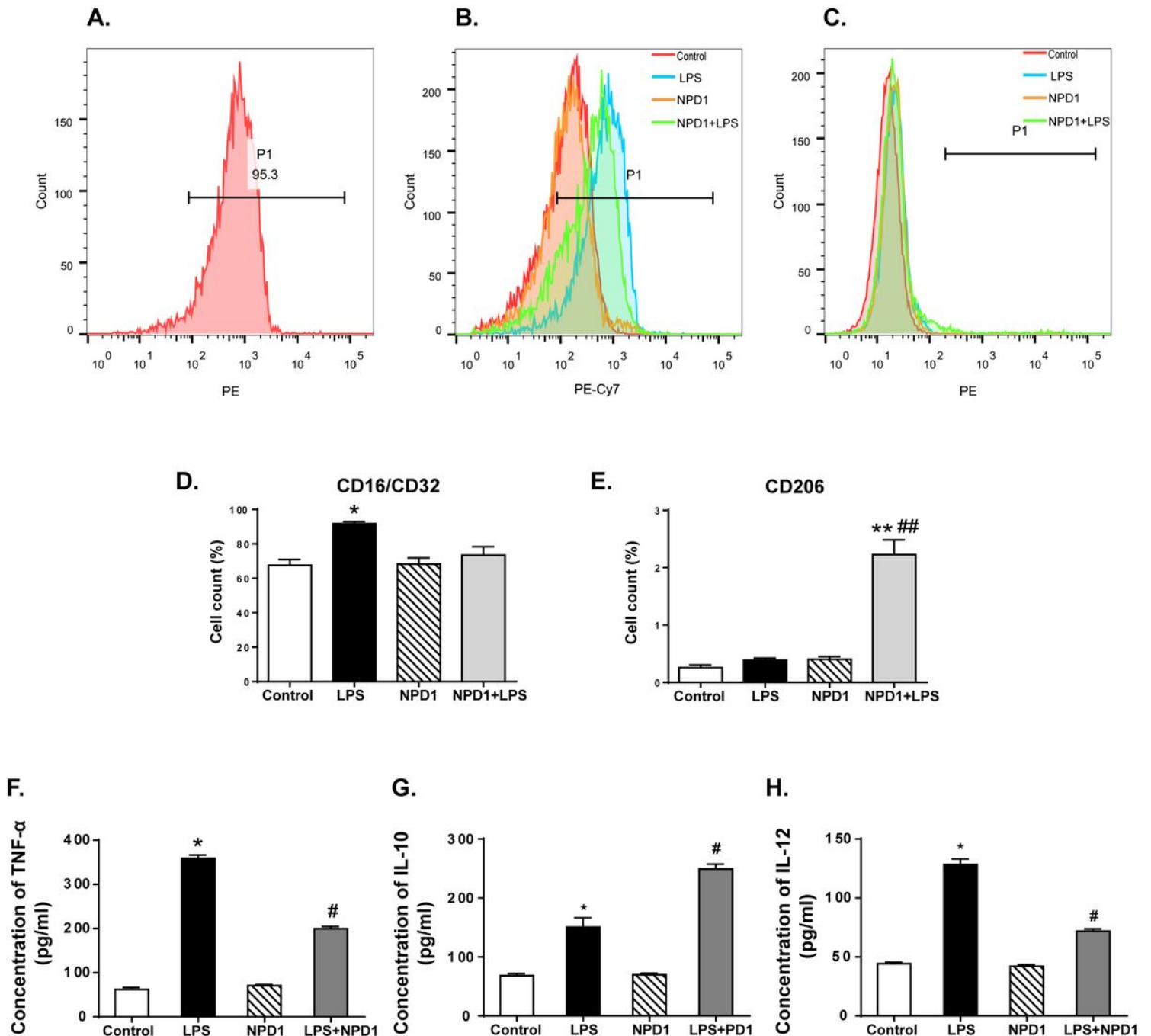


**Figure 6**

NPD1 promotes the macrophage polarization to M2 phenotype after proinflammatory stimulation on BMDMs, and modulates the expression of inflammatory cytokine profile. The expression of macrophage marker CD68 was showed in (A). NPD1 promoted the transformation of BMDMs cell markers from M1 to M2 phenotype, as measured by flow cytometry (B-C). The ratio of M1 and M2 phenotype in different

groups was calculated (D-E). The concentration of tumor necrosis factor- $\alpha$  (TNF- $\alpha$ ), IL-12 and IL-10 were tested by ELISA (F-H). Data are presented as means  $\pm$  SEM of the mean for each group (n = 5 per group). \*P < 0.05 versus the Control group, \*\*P < 0.01 versus the Control group, #P < 0.05 versus the Surgery group.